RSC Advances

ROYAL SOCIETY
OF CHEMISTRY

www.rsc.org/advances

Cite this: DOI: 10.1039/c0xx00000x

www.rsc.org/xxxxxx

ARTICLE TYPE

Facile synthesis of polyaniline/carbon dots nanocomposites and application as fluorescent probe to detect mercury

Xiufang Wang*[a], Jun Zhang[a], Wensheng Zou[a], and Runxia Wang[b]

Received (in XXX, XXX) Xth XXXXXXXXX 20XX, Accepted Xth XXXXXXXXX 20XX

DOI: 10.1039/b000000x

In this work, for the first time, novel polyaniline/carbon dots (PANI/Cdots) nanocomposites have been synthesized by a simple method. Meanwhile, the bright fluorescence of Cdots is effectively quenched by PANI through fluorescence resonance energy transfer. With the addition of Hg^{2+}, the strong binding ability between Hg^{2+} and amino groups of PANI makes the Cdots be released break away from the PANI, resulting in restoration of Cdots fluorescence, which constructs a fluorescent probe for Hg^{2+} detection. This fluorescence "off-on" signal is sensitive to the concentration of Hg^{2+}, and there is a good linear relationship between the fluorescence intensity of Cdots and the Hg^{2+} concentrations in the range from 0.05 to 1.0 µM. The detection limit for Hg^{2+} at a concentration is 0.8 nM. Moreover, it turns out that the nanoprobes represent a rather high selectivity for Hg^{2+} detection. We believe the PANI/Cdots composites will emerge a new class of fluorescence materials that could be very likely to be suitable for practical application.

1. Introduction

Mercury (II) ion (Hg^{2+}) is a hazardous environmental contaminant due to its accumulative and high toxic properties and causes harm to the human body mainly via the central nervous system, digestive system and internal organs.[1] Even in low concentration, it is a threat to the environment and human health because mercury is non-biodegradable and can enter food chain. The maximum allowable level of Hg^{2+} defined by United States Environmental Protection Agency is 10 nM in drinking water.[2] So various sensors have been developed for the detection of Hg^{2+}, including colorimetry, photoelectrochemistry, atomic absorption/emission spectroscopy, electrochemical techniques, SERS spectroscopy and so forth.[3-7] But it is still of great challenge to develop new methods for aqueous Hg^{2+} analysis with high sensitivity, selectivity and simplicity.

Because of their ultrasensitivity, rapid and easy operations, in recent years, much effort has been devoted to develop fluorescent sensors derived from various nanomaterials including gold clusters, silica nanoparticles, polymer nanoparticles, carbon dots, graphene oxide, and graphene quantum dots etc.[8-14] Among these fluorescent materials, Cdots have recently received much attention due to their many unique and novel properties. Compared with conventional semiconductor nanodots and organic dyes, Cdots have good water solubility, low cytotoxicity, robust chemical inertness, low photobleaching, cost effectiveness, and excellent biocompatibility etc.[15] They have broad application prospects in many technologies, such as bioimaging, sensing, photocatalysis, fluorescent ink.[16-19] So far, a variety of simple, fast, and cheap synthetic routes to prepare Cdots, such as pyrolysis, combustion, hydrothermal process, template, electrochemistry, ultrasonic and microwave synthesis.[20-26] Cdots display photoluminescence properties reminiscent of those of quantum dots which are widely used as energy donors in fluorescence resonance energy transfer (FRET) applications.[27] Cdots as a new class of fluorescent nanomaterials are expected to behave as better FRET donors and acceptors than other organic fluorescent molecules. However, research on FRET using Cdots is still in the initial stages and there have been few reports concerning the potential applications of such materials. As a consequence of the health concerns and the known environmental and biological hazards of Cdots, Cdots are at the center of significant research efforts to develop novel FRET sensors.

PANI is a very important polymer, and it is also the most extensively investigated conducting polymer in recent years, owing to its facile and low cost synthesis, good environmental stability, nontoxicity, reversible electrochemistry, corrosion protection, and high instinct redox properties etc.[28] It has large variety of applications such as sensors, electrochromic devices, secondary batteries, catalysis and electrostatic discharge protection.[7, 29-32] On the other hand, PANI is also a class of aromatic conjugated polymers with rigid, plane π-π electronic conjugated system, showing absorption in the region of ultraviolet and visible light. So it should be a quencher of Cdots, as a result of nonradiative transfer of electronic excitation energy from Cdots excited states to its π system. Inspired by this property, PANI may be used as FRET acceptors with Cdots as energy donors, in which PANI exhibits high efficiency in quenching the donor emission and consequently provides good sensitivity. Hence, this has made it possible and important to establish FRET systems using PANI/Cdots nanocomposites.

Here, we have been synthesized PANI/Cdots nanocomposites by a simple method and established a novel FRET system. With the addition of Hg^{2+} into the system, the quenched fluorescence of Cdots has been restored. This fluorescence “off-on” signal is sensitive to the concentration of Hg^{2+}, and there is a good linear relationship between the fluorescence intensity of Cdots and the Hg^{2+} concentration. The detection limit for Hg^{2+} at a concentration is 0.8 nM. The PANI/Cdots probe is also successfully applied to the determination of Hg^{2+} ions in real water samples. To the best of our knowledge, this work represents the first example based on PANI/Cdots nanocomposites for Hg^{2+} detection and it would have great potential applications in the Hg^{2+} monitoring of environment and food.

2. Results and discussion

2.1. Synthesis and characterization of PANI/Cdots compsites

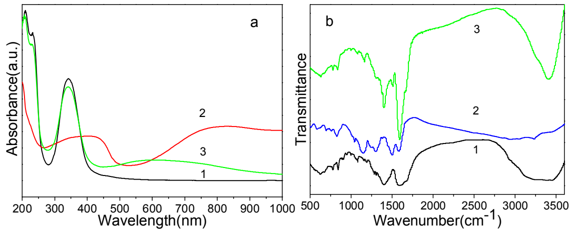

Fig. 1 UV-vis (a) and FTIR (b) spectra of Cdots (1), PANI (2), and PANI/Cdots (3).

The UV-vis absorption spectra of as-prepared samples are shown in Fig. 1a. The Cdots solution has an absorption peak at 340 nm and a feature at 235 nm in the UV–vis absorption spectrum of Cdots (curve1). The UV-vis absorption spectrum of PANI is shown in curve 2 (Fig 1a). Two bands at about 420 nm, and 760 nm observed in the UV-vis absorption spectrum of the samples are attributed to the π-π* transition and the exciton-like transition from the benzenoid rings, to the quinoid rings, respectively, which are consistent with the formation of the conventional emeraldine base, indicating the prepared PANI is in a proton doped state with positive electricity on the surface of moleculars.[33] In the UV-vis absorption spectrum of PANI/Cdots composite (curve 3), the absorption peaks have some changes, except for the absorption peak of Cdots at 340 nm. The peak of PANI at 420 nm is not observed, which may be overlapped by that of Cdots. The band at 760 nm moves to 590 nm. These all show that there are interactions between PANI and Cdots.

Fig. 1b is FTIR spectra of the prepared samples. For the Cdots (curve 1), the peaks at 1580 and 1396 cm^{-1}correspond to the asymmetric and symmetric stretching vibrations of the carboxylate anions, respectively. Bands at 3200–3600 cm^{-1} are attributed to the stretching vibration of hydroxyl groups. The results reveal that carboxylate with negative electricity and hydroxyl groups are mainly on the surface of Cdots. In the spectrum of pure PANI (curve 2), the characteristic peaks at 1579 and 1491 cm^{-1} are due to the C=C stretching vibration of quinoid and benzenoid rings, respectively, and peaks at 1297 and 1235 cm^{-1} are related to the C-N and C=N stretching modes. The bands at 1143 and 819 cm^{-1} are the distinctive features of C-H in-plane and C-H out-of-plane bending, respectively. The FTIR spectrum of the PANI/Cdots composite shows all the bands of PANI and Cdots (curve 3). However, it can be found that there are also some changes compared with pure PANI and Cdots. The intensity of some peaks in the composite is lower than that of pure PANI, while the intensity of the peak of Cdots at 1580 cm^{-1} decrease, which further confirms that there are interactions between PANI and Cdots in the composite.

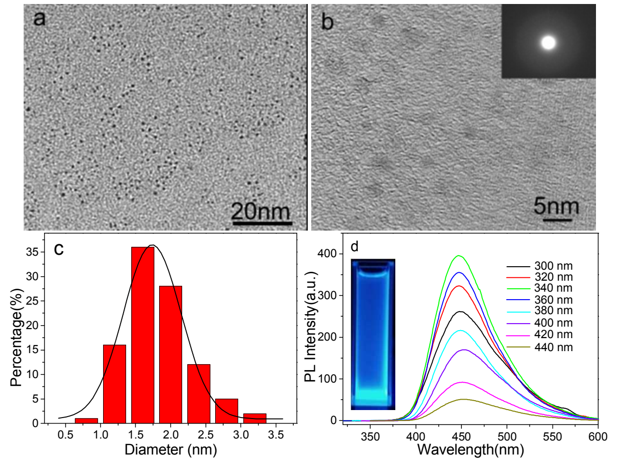

Fig. 2 (a) TEM and (b) HRTEM images of synthesized Cdots, insets in (b): SAED pattern of the Cdots, (c) size distribution, and (d) FL spectra of Cdots excited by different wavelength, inset photograph of the Cdots solution under UV lamp λex = 365 nm.

The morphology of the Cdots is investigated by TEM. From Fig. 2a, it can be clearly seen that the as-synthesized Cdots are uniform in size and possess a nearly spherical shape. No obvious lattice fringes are found in the high resolution HRTEM of the Cdots (Fig. 2b), which is indicative of their amorphous nature. The indiscernible diffuse rings in the selected-area electron-diffraction pattern (inset in Fig. 2b,) further confirm the poor crystallization of the Cdots. Cdots have a narrow size distribution. Fig. 2c reveals that the average size of the Cdots is about 1.7 nm. The Cdots solution exhibits strong bright blue luminescence under excitation of 365 nm, which can be easily seen with the naked eye and recorded with a digital camera, as shown in the inset (Fig.2d). The emission peaks of Cdots at various excitation wavelengths from 300 to 440 nm are shown in Fig. 2d. It is noted that with the increasing of excitation wavelength, the intensity of luminescence increases to the maximum (340 nm excitation), then decreases. The full width at half-maximum is about 68 nm. The peaks do not shift, indicating that the luminescence origin of Cdots might be different from most other Cdots that show the excitation wavelength dependent fluorescence. The maximum emission wavelength at different excitation wavelengths remains at 448 nm. Therefore, 340 nm is selected as the excitation wavelength for the following experiments.

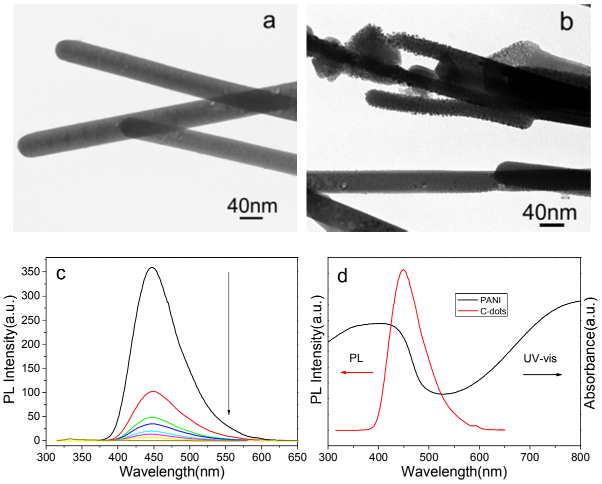

Fig. 3 TEM images of PANI (a), PANI/Cdots composite (0.28:0.20, v/v) (b), the fluorescence quenching of Cdots with the different volume ratio of PANI/Cdots, (from top to bottom: 0:0.2, 0.04:0.2, 0.08:0.2, 0.12:0.2, 0.16:0.2,0.2:0.2, 0.24:0.2, and 0.28:0.2) (c) and Photoluminescence (red) and UV-vis spectra (black) of Cdots and PANI (d).

As shown in Fig. 3a, the synthesized PANI is uniform nanofibers, and the surface of nanofibers is very smooth. The average diameter of PANI is about 40 nm and length is several micrometers. When PANI with positive charge and carboxyl group functionalized Cdots are mixed in aqueous solution, the Cdots have been successfully attached onto the surface of PANI nanofibers through electrostatic interactions and do not aggregate (Fig. 3b). So the TEM analyses confirm the formation of PANI/Cdots nanocomposite.

When the Cdots and PANI are mixed, the fluorescence of Cdots is quenched in direct proportion to the volume ratio of PANI/Cdots (denoted by X), (Fig. 3c). When the X is 0.04:0.2, the fluorescence intensity of Cdots is quenched about 72%. With the further increase of X to 0.28:0.2, over 98% of fluorescence is quenched and reaches to an equilibrium value, and the bright blue fluorescence under UV lamp disappeared. For assays based on such a fluorescence off-on model, higher quenching rates are generally preferable in terms of detection sensitivity. Here, PANI with positive charge helps to attach carboxyl-stabilized Cdots. The highly efficient quenching by PANI should originate from the FRET from PANI to Cdots owing to spectral overlapping. The absorption spectrum of PANI and emission spectrum of aqueous Cdots solution under excitation at 340 nm are shown in Fig. 3d, and the emission peak of Cdots is about at 448 nm. While, the PANI exhibits absorption centered at 420 nm, which has a partial spectral overlap with the Cdots emission. The spectral relationship indicates that the adsorption of Cdots at the surface of PANI may lead to highly efficient quenching of Cdots fluorescence by FRET.

2.2. PANI/Cdots fluorescent probe for detection of Hg^{2+}

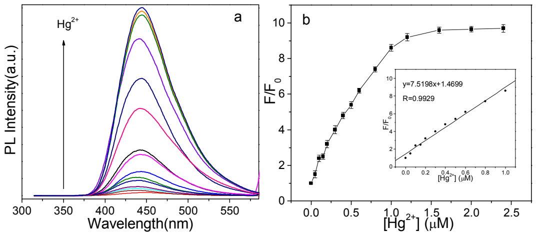

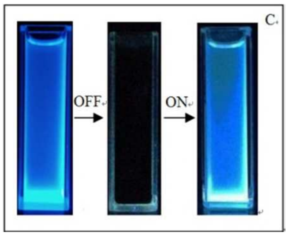

Fig. 4 (a) Evolution of fluorescence spectra of PANI/Cdots (0.28:0.20, v/v) with the addition of Hg^{2+}(0, 0.05, 0.1, 0.15, 0.2, 0.3, 0.4, 0.5, 0.6, 0.8, 1.0, 1.2, 1.6, 2.0 and 2.4 μM), (b) Plot of the fluorescence intensity vs Hg^{2+} concentration (the insert is linear correlation), and (c) Photographs of the PANI/Cdots solution in the fluorescence off-to-on process under a 365 nm UV lamp.

Based on above fluorescent properties of PANI/Cdots nanocomposite, we explored the feasibility of using the as-prepared PANI/Cdots for Hg^{2+} detection. As shown in Fig. 4a, it can be seen that the fluorescence of Cdots continuously recovers with the addition of Hg^{2+} to the PANI/Cdots solution. The fluorescence enhancement is closely related to the amount of Hg^{2+} added to the PANI/Cdots probe solution. About 8.7-fold fluorescence enhancement is measured when the concentration of Hg^{2+} reaches 1.0 μM. Even if Hg^{2+} concentration is as low as 0.05 μM, the fluorescence intensity is still enhanced ca.1.5-fold. Fig. 4b shows the plot of fluorescence enhancement percentage vs the concentration of Hg^{2+}. As shown in the insert, the best linear response concentration range of Hg^{2+} is from 0.05 to 1.0 μM, while the quantification of Hg^{2+} can be achieved with standard deviation $R = 0.9929$., and the lowest detection limit (LOD) is about 0.8 nM based on the standard deviation of the response (σ) and the slope of the calibration curve (S) at levels approximating the LOD according to the formula: LOD = 3.3(σ/S), which is lower than the previously reported results.[34] Notably, the ultrasensitive detection of Hg^{2+} using the novel probe can be achieved in the aqueous solution.

The effect of pH on the fluorescence recovery of the sensor system was studied with concentration of Hg^{2+} 0.8 nM. The results show that there is slight variation of the value of F/F_0 in the pH range of 2.0–9.0 (Fig. S1). So the sensor system has a wide pH range for Hg^{2+} detection.

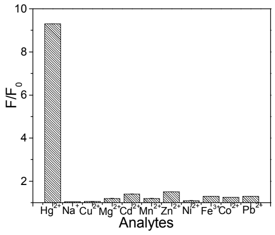

Fig. 5 Selectivity investigation of the PANI/Cdots probe for Hg^{2+} detection (ions concentration: 20 μM).

In order to evaluate the selectivity of PANI/Cdots probe to Hg^{2+}, the fluorescence response in the presence of 10 other metal common ions were also investigated including Na^{+}, Cu^{2+}, Mg^{2+}, Cd^{2+}, Mn^{2+}, Zn^{2+}, Ni^{2+}, Fe^{3+}, Co^{2+}, and Pb^{2+}. As shown in Fig. 5, only Hg^{2+} ions could significantly enhance the ratiometric luminescence output of PANI/Cdots. The fluorescence intensity of PANI/Cdots composite remains almost unchanged upon adding metal ions, such as Na^+, Mg^{2+},Cu^{2+}, Fe^{3+}, Co^{2+}, Ni^{2+}, Mn^{2+}, and Pb^{2+}. In addition, the slight fluorescence enhancement can be observed upon addition of Cd^{2+} and Zn^{2+} to PANI/Cdots composite, this is because Cd^{2+} and Zn^{2+} have the same electronic configuration and similar chemical properties to Hg^{2+}, and they can react with N atoms in PANI polymeric chains to form the corresponding complex. However, the slight fluorescence enhancement of Cd^{2+} and Zn^{2+} in this study does not affect the application of the present PANI/Cdots probe in Hg^{2+} detection. According to literatures,[7] the main adsorption sites for metal ions are the nitrogen atoms in the PANI chains because the nitrogen atom has a lone pair of electrons that can bind a metal ion to form a metal complex. Compared with other metal ions, Hg^{2+} has larger ionic radius, and the polarization and deformation happen more easily when they interact with nitrogen atoms of PANI. So the high selectivity of PANI/Cdots probe for Hg^{2+} may be due to that Hg^{2+} ion has higher thermodynamic affinity and faster chelating process with "N" of PANI than other metal ions. These results suggest that the PANI/Cdots probe exhibits a high selectivity to Hg^{2+}. A reasonable explanation for high selectivity to Hg^{2+} needs to be further discussed.

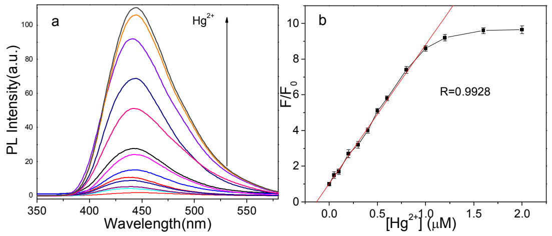

Fig. 6 FLuorescence response of PANI/Cdots in presence of lake water containing different concentrations of Hg^{2+} (0, 0.05, 0.1, 0.2, 0.3, 0.4, 0.5, 0.6, 0.8, 1.0, 1.2, 1.6, 2.0 μM), (b) Plot of the fluorescence intensity vs Hg^{2+} concentrations.

The practical application of the designed probe for detecting Hg^{2+} in river water samples was also tested. To evaluate the PANI/Cdots probe in anartificial system, the performance of the present probe for real water sample analysis was conducted by lake water samples obtained from the Caohu of Hefei, Anhui province, China. First, the water sample was filtered to get rid of any insolubles. Subsequently, standard Hg^{2+} solutions with different concentrations were added to the pretreated water sample, and then analyzed with the proposed method. Fig. 6 shows the fluorescence response of PANI/Cdots in presence of lake water containing different concentrations of Hg^{2+} ions (a), and the corresponding relationship between fluorescence intensity and the concentrations of Hg^{2+} (b). It can be seen that the fluorescence intensity gradually recoveres with increasing the concentration of Hg^{2+} in lake water from 0 to 1.2 μM. The calibration curve for determining Hg^{2+} in the lake water are obtained by plotting the values of F/F_0 versus the concentrations of Hg^{2+}. As shown in Fig. 6b, a good linear correlation has been obtained in the range of 0–1.0 μM for the lake water. The results indicate that the PANI/Cdots probe may be a promising sensing platform for the detection of Hg^{2+} in real environmental samples.

Fluorescence "off-to-on" mechanism for Hg^{2+} Detection

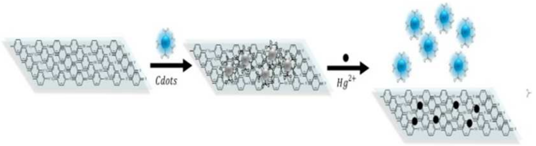

Scheme 1 Fluorescence "off-to-on" mechanism for the detection of Hg^{2+}.

Scheme 1 illustrates the fluorescence off-to-on mechanism of PANI/Cdots probe for the detection of Hg^{2+}. Here, Cdots have been used as energy donors, while PANI is FRET acceptors. PANI possesses π－π stacking and amino with positive charge, while the surface of Cdots has negative charge because of carboxyl groups, which all bring the donor (Cdots) and the acceptor (PANI) into close proximity (Fig. 3b). So the emission of Cdots has been effectively quenched by PANI through FRET, and it consequently provides good sensitivity. In the presence of Hg^{2+}, the binding between amino groups of PANI and Hg^{2+} disturb the interaction between the Cdots and PANI. Such interactions release the Cdots from the PANI (Fig. S2), resulting in restoration of Cdots fluorescence (Fig. 4c). This design results in a fluorescence-enhanced detection that is sensitive and selective to Hg^{2+}.

3. Experimental section

3.1. Materials

Aniline monomer, ammonium persulfate, sodium citrate, and ammonium bicarbonate were all analytical-grade reagents (Shanghai Chemical Reagent Co. Ltd., China). The other reagents were used as received without further purification. Double distilled water was used throughout the experiment to prepare the solutions.

3.2. Synthesis of Cdots

Cdots were prepared according to a previously described method.[35] Briefly, sodium citrate (0.2 g), NH_4HCO_3 (1.5 g) and water (10mL) were sealed into a Teflon equipped stainless steel autoclave, which was then placed in a drying oven followed by hydrothermal treatment at 180 ℃ for 4 h. After the reaction, the autoclave was cooled to room temperature. The purification of the Cdots was conducted through a dialysis tube (1000 Da, molecular weight cutoff) for about 24 h in dark. The final Cdots with the end group of carboxylic acid were redispersed in Cdots with the concentration of 2 mg/mL for the further application.

3.3. Preparation of PANI

In a typical synthesis, APS (0.22 g, 0.965 mmol) was dissolved in 8 mL of deionized water to prepare an oxidant solution at room temperature. The oxidant solution was then added dropwise to the aniline monomer (0.03 mL, 0.322 mmol) solution. Then the reaction mixture was continuously stirred for 6 h in a water bath at room temperature. Finally, the polymerization system was immobilized for 48 h at 0-5 ℃. The remaining precipitate was washed several times with deionized water, and ethanol, and then dried under vacuum for 24 h at 50 ℃. The powder of PANI was redispersed to get a solution with a concentration of about 6 mg/mL.

3.4. Formation of PANI/Cdots composite

0.2 mL of Cdots solution and a certain volume of PANI dispersions (0, 0.04, 0.08, 0.12, 0.16, 0.2 and 0.24 mL) were mixed with deionized water in a centrifuge tube with the final volume of 2 mL, and incubated for 30 min at room temperature before fluorescence measurement. Then the fluorescence spectra were measured in a 2 mL quartz cuvette at room temperature.

3.5. Detection of Hg^{2+}

A typical procedure for the detection of Hg^{2+} is described as follows: the fluorescence spectrum of 2 mL PANI/Cdots suspension (PANI/Cdots: 0.28:0.20, v/v) was recorded subsequently and the fluorescence intensity was set as F_0. Then, different concentrations of Hg^{2+} (0, 1.0, 2.0, 4.0, 6.0, 10.0, 15.0, 20.0, 30.0, 50.0, and 100.0 mM) were mixed with the above solution under gentle shaking. The corresponding fluorescence spectra were recorded and a series of F/F_0 values were obtained. The other metal ions, such as Na^+, Mg^{2+},Cu^{2+}, Cd^{2+}, Fe^{3+}, Co^{2+}, Ni^{2+}, Mn^{2+}, Pb^{2+}, Zn^{2+}, etc., were also measured. All the detection experiments were carried out under the same conditions at room temperature. To evaluate the PANI/Cdots-based sensor for Hg^{2+} detection in a practical application, the performance of the present method for real water sample analysis was examined by lake water samples from Caohu (Anhui,China). The lake water samples were filtered through a 0.20 μm filtered membrane and centrifuged at 10,000 rpm for 10 min to get rid of any insolubles. The lake water samples were added Hg^{2+} at different concentration levels and analyzed with the proposed method.

3.6. Characterization

UV-vis absorption spectra were recorded at room temperature by a TU-1800PC spectrometer. FTIR spectra were obtained using a NEXUS-870 spectrophotometer (frequency range from 3600 to 400 cm^{-1}) with KBr pellet. SEM was examined using a JSM-7500F field-emission scanning electron microscope. TEM was performed by using a JEM-2100F instrument with a field emission gun operating at 200 kV. The fluorescence spectra were recorded at room temperature on an F-7000 fluorescence spectrophotometer (Hitachi) with a quartzcell (1mm). Both the excitation and emission slit widths were fixed at 5 nm. Photographs were taken with a canon 350D digital camera.

4. Conclusions

In conclusion, we have developed a PANI/Cdots "off–on" fluorescent probe for the simple, ultrasensitive and selective detection of Hg^{2+} in aqueous media. The PANI/Cdots composites are prepared via the electrostatic interaction. Meanwhile, the fluorescence of Cdots is effectively quenched by FRET. The fluorescence intensity of Cdots is switched on with the addition of Hg^{2+}. A good linear fit between the fluorescence response and Hg^{2+} concentration is obtained in the range 0.05 to 1.0 μM. The LOD is found to be 0.8 nM for Hg^{2+}. In addition, the probe shows a high selectivity for Hg^{2+} over other metal ions. Most importantly, the PANI/Cdots exhibits promising application of Hg^{2+} detection for real-water samples. Thus, it is believed that the present strategy may offer a new approach for developing low-cost, high sensitive and selective Hg^{2+} sensors in environmental applications.

Acknowledgment

This work was supported by the Natural Science Foundation of Anhui Province (1308085MB29, 1308085QB33, 1408085MB27), the Natural Science Foundation of China (21301004, 21201005), the Natural Science Foundation of Anhui Educational Committee (KJ2014ZD080), and China Postdoctoral Science Foundation funded project (2013M5418100, 2013M530301).

Notes and references

[a] *Anhui Key Laboratory of Advanced Building Materials, Anhui Jianzhu University, Hefei Anhui, P.R. China, 230601, Tel.: +86 551 63828100; fax: +86 551 63828100; E-mail:wxfrye159@sina.com*
[b] *Pharmacy department, Anhui Medical College, Hefei Anhui, P.R. China, 230601*

1 R. Z. Zhang and W. Chen, *Biosens. Bioelectron.*, 2014, **55**, 83-90.
2 EPA, U.S., Mercury Update: Impact on Fish Advisories. EPA Fact Sheet EPA-823-F-01-011; EPA, Office of Water: Washington, DC, 2001.
3 N. Kanayama, T. Takarada and M. Maeda, *Chem. Commun.*, 2011, **47**, 2077-2079.
4 B. T. Zhang and L. H. Guo, *Biosens. Bioelectron.* 2012, **37**, 112-115.
5 J. V. Cizdziel and S. Gerstenberger, Talanta, 2004, **64**, 918-921.
6 S. Tang, P. Tong, J. F. Chen, Z. M. Yan and L. Zhang, *Biosens. Bioelectron*., 2014, **59**, 1-5.
7 X. F. Wang, Y. H. Shen, A. J. Xie, S. K Li, Y.. Cai, Y. Wang and H. Y. Shu, *Biosens. Bioelectron.*, 2011, **26**, 3063-3067.
8 C. V. Durgadas, C. P. Sharma and K. Sreenivasan, *Analyst*, 2011, **136**, 933-940.
9 U. H. F. Bunz and V. M. Rotello, *Angew. Chem., Int. Ed.*, 2010, **49**, 3268-3279.
10 X. Wang, C. Boschetti, M. J. Ruedas-Rama and E. A. H. Hall, *Analyst*, 2010,**135**, 1585-1591.
11 Y. Mao, Y. Bao, D. X. Han, F. H. Li and L. Niu, *Biosens. Bioelectron.*, 2012, **38**, 55-60;
12 Q. S. Mei and Z. P. Zhang, *Angew. Chem., Int. Ed.*, 2012, **51**, 5602-5606.
13 J. Ju, R. Z. Zhang, S. J. He and W. Chen, *RSC Adv.*, 2014, **4**, 52583-52589.
14 J. Ju and W. Chen, *Biosens. Bioelectron*., 2014, **58**, 219-225.
15 Y. M. Guo, L. F. Zhang, S. S. Zhang, Y. Yang, X. H. Chen and M. C. Zhang, *Biosens. Bioelectron.*, 2015, **63**, 61-71.
16 B. Kong, A. Zhu, C. Q. Ding, X. M. Zhao, B. Li and Y. Tian, *Adv. Mater.*, 2012, **24**,5844-5848.
17 S. J. Zhu, J. H. Zhang, L. Wang, Y. B. Song, G. Y. Zhang and H. Y. Wang, *Chem. Commun.*, 2012, **48**, 10889-10891.
18 Y. Xu, M. Wu, X. Z. Feng, X. B. Yin, X. W. He and Y. K. Zhang, *Chem. Eur. J.*, 2013, **19**, 6282-6288.
17 S. J. Zhu, Q. N. Meng, L. Wang, J. H. Zhang, Y. B. Song and H. Jin, *Angew. Chem. Int. Ed.*, 2013, **52**, 3953-3957.
120 P. C. Hsu and H. T. Chang, *Chem. Commun*., 2012, **48**, 3984-3986.
21 Z. Xie, F. Wang and C. Y. Liu, *Adv. Mater.*, 2012, **24**, 1716-1721.
22 L. Bao, Z. L. Zhang, Z. Q. Tian, L. Zhang, C. Liu and Y. Lin, *Adv. Mater.*, 2011, **23**, 5801-5806.
23 H. T. Li, X. D. He, Y. Liu, H. Huang, S. Y. Lian and S. T. Lee, *Carbon*, 2011, **49**, 605-609.
24 L. Q. Liu, Y. F. Li, L. Zhan, Y. Liu and C. Z. Huang, *Sci. China. Chem.*, 2011, **54**, 1342-1347.
25 J. Zong, Y. H. Zhu, X. L. Yang, J. H. Shen and C. Z. Li, *Chem. Commun.*, 2011, **47**, 764-766.
26 H. P. Liu, T. Ye and C. D. Mao, *Angew. Chem.*, 2007, **119**, 6593-6595.
27 K. E. Sapsford, L. Berti and I. L. Medintz, *Angew. Chem. Int. Ed.* 2006, **45**, 4562-4589.
28 F. Chen and P. Liu, *ACS Appl. Mater. Interfaces*, 2011, **3**, 2694-2702.
29 F. D. R. Amado, M. A. S. Rodrigues, F. D. Morisso, A. M. Bernardes, J. Z. Ferreira and C. A. Ferreira, *J. Collod. Interface Sci.*, 2008, **320**, 52-61.

30 Y. Qiao, S. J. Bao, C. M. Li, X. Q. Cui, Z. S. Lu and J. Guo, *ACS Nano.*, 2008, **2**, 113-119.
31 J. Alam, L. A. Dass, M. S. Alhoshan and A. W. Mohammad, *Appl. Water. Sci.*, 2012, **2**, 37-46.
32 S. Radhakrishnan, C. R. Siju, D. Mahanta, S. Patil and G. Madras, *Electrochem. Acta*, 2009, **54**, 1249-1254.
33 X. M. Feng, C. J. Mao, G. Yang, W. H. Hou and J. J. Zhu, *Langmuir,* 2006, **22**, 4384-4389.
34 X. Cui, L. Zhu, J. Wu, Y. Hou, P. Y. Wang, Z. N. Wang and Mei Yang, *Biosens. Bioelectron.*, 2015, 63, 506-512.
35 Y. M. Guo, Z. Wang, H. W. Shao and X. Y. Jiang, *Carbon*, 2013, **52**, 583-589.

TOC graphic

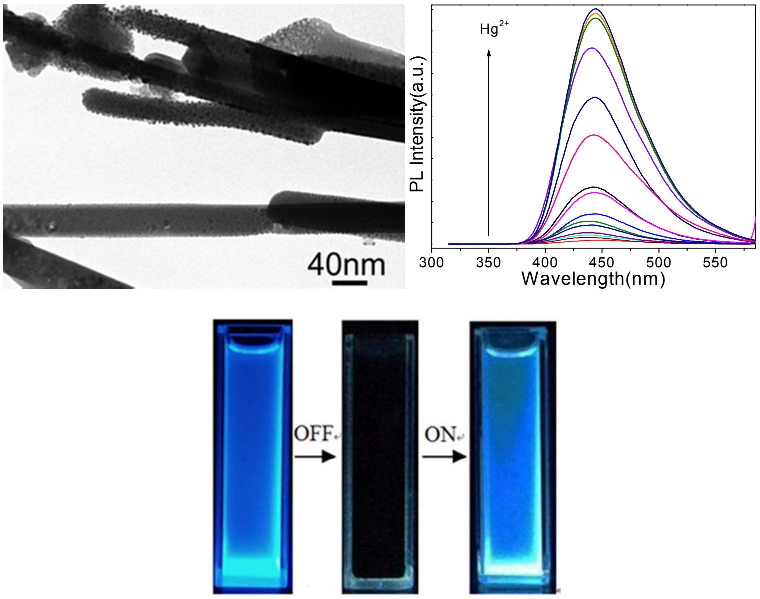

TOC synopsis

Novel polyaniline/carbon dots nanocomposites have been synthesized by a simple method, and a PANI/Cdots "off–on" fluorescent probe has been constructed for the simple, ultrasensitive and selective detection of Hg^{2+} in aqueous media.